

Analysis of the dispersion function for anisotropic longitudinal plasma waves

M. D. Arthur, R. L. Bowden, and P. F. Zweifel

Citation: *Journal of Mathematical Physics* **20**, 2126 (1979); doi: 10.1063/1.523982

View online: <http://dx.doi.org/10.1063/1.523982>

View Table of Contents: <http://scitation.aip.org/content/aip/journal/jmp/20/10?ver=pdfcov>

Published by the [AIP Publishing](#)

An advertisement banner for Maple 18. The background is a dark blue gradient with abstract, glowing light blue and purple geometric shapes. On the left, there is a red arrow pointing right with the text 'Now Available!'. Below this, the 'Maple 18' logo is displayed in large, bold, blue and red letters, with the tagline 'The Essential Tool for Mathematics and Modeling' underneath. On the right side, the text 'State-of-the-art environment for algebraic computations in physics' is written in white. Below this, a list of four bullet points describes the new features. At the bottom right, there is a blue button with the text 'Read More' in white.

Now Available!

Maple™ 18

The Essential Tool for Mathematics and Modeling

State-of-the-art environment for algebraic computations in physics

- More than 500 enhancements throughout the entire Physics package in Maple 18
- Integration with the Maple library providing access to Maple's full mathematical power
- A full range of physics-related algebraic formulations performed in a natural way inside Maple
- World-leading tools for performing calculations in theoretical physics

[Read More](#)

Analysis of the dispersion function for anisotropic longitudinal plasma waves^{a)}

M. D. Arthur, R. L. Bowden, and P. F. Zweifel

Laboratory for Transport Theory and Mathematical Physics, Virginia Polytechnic Institute and State University, Blacksburg, Virginia 24061

(Received 24 April 1979; accepted for publication 1 June 1979)

An analysis of the zeros of the dispersion function for longitudinal plasma waves is made. In particular, the plasma equilibrium distribution function is assumed to have two relative maxima and is not necessarily an even function. The results of this analysis are used to obtain the Wiener–Hopf factorization of the dispersion function. A brief analysis of the coupled nonlinear integral equations for the Wiener–Hopf factors is also presented.

I. INTRODUCTION

The solution of boundary value problems (fixed frequency waves) as described by the linearized Vlasov equation requires the Wiener–Hopf factorization of the plasma dispersion function A .^{1,2} For the longitudinal modes which we consider in the present paper, the relevant Vlasov–Maxwell set of equations (in the absence of magnetic fields) can be taken to be

$$\frac{\partial g}{\partial t} + u \frac{\partial g}{\partial z} + \frac{e}{m} (E_A + E) F'(u) = 0, \quad (1a)$$

$$\frac{\partial E}{\partial t} = -4\pi n_0 e \int_{-\infty}^{\infty} s g(z, s, t) ds. \quad (1b)$$

Here, u represents the longitudinal electron velocity, F is the equilibrium distribution function, g is the deviation of the distribution function from equilibrium, E_A is the applied electric field (z component), E is the z component of the self-consistent electric field, and n_0 is the plasma density. We might note that in the previous analyses, Refs. 1 and 2, it has been customary to use Gauss' Law, instead of Ampere's Law [Eq. (1b)]. After Fourier-transforming in the time variable, this leads to a set of two coupled equations for f_ω and E_ω ($f_\omega(z, u) = \int_{-\infty}^{\infty} e^{i\omega t} g(z, u, t) dt$). Since it is much easier to work with a one-component equation, we choose to begin our analysis with Ampere's Law.

Thus, after the aforementioned Fourier transformation, the equation we study is

$$\frac{\partial f}{\partial z} + i\omega K f = -\frac{e}{i\omega m} E_A \frac{F'(u)}{u}, \quad (2a)$$

with the unbounded linearized operator K defined by

$$(Kf)(z, u) = \frac{1}{u} f(z, u) + \sigma^2 \frac{F(u)}{u} \int_{-\infty}^{\infty} s f(z, s) ds \quad (2b)$$

(we will henceforth not explicitly exhibit the dependence of f on the frequency ω). Here, $\sigma^2 = \omega_p^2/\omega^2$, where $\omega_p^2 = 4\pi n_0 e^2/m$ is the plasma frequency.

The dispersion function associated with the eigenvalues of K is found to be

$$\Omega(\rho) = 1 + \sigma^2 \int_{-\infty}^{\infty} \frac{s F'(s)}{1 - s\rho} ds,$$

and is related to the dispersion function A of Refs. 1 and 2 by $A(\rho) = \Omega(1/\rho)$

$$A(\rho) = 1 - \sigma^2 \rho \int_{-\infty}^{\infty} \frac{s F'(s)}{s - \rho} ds. \quad (3)$$

In subsequent papers currently in preparation, we consider the uniqueness of solutions to Eq. (2a) and construct explicit solutions. In the present paper we study A .

For the case that F is isotropic, it is well known^{1,2} that A has no zeros if $\sigma^2 < 1$; K then has no eigenvalues, and the plasma waves are dissipative. However, we are interested in anisotropic plasmas, for example, the "bump on tail" or "two stream" equilibria,³ for which eigenvalues may indeed exist.

In Sec. II we discuss the zeros of A . In Sec. III we present the Wiener–Hopf factorization of A by analytic functions X and Y . In Sec. IV we obtain the coupled nonlinear integral equations for these functions and discuss their solutions. Our analysis is then in generalization of the isotropic case considered, for example, in Ref. 3.

II. ZEROS OF A

The zeros of the plasma dispersion function for fixed k ($\omega_0 = \omega_0(k)$) have been studied extensively (cf., for example, Ref. 3, Chap. 7). Since our interest is in plasma wave boundary value problems rather than the stability of solutions to the initial value problem, we need $k_0(\omega)$, i.e., the zeros for fixed frequency ω . In this section we sketch the procedure we have used for locating the half-plane in which these zeros can occur and quote the results for "bump on tail" and "two stream" equilibrium distributions. Our procedures can easily be generalized to more complicated equilibrium distributions if desired.

We observe that the zeros occur in complex conjugate pairs. Thus it is sufficient to consider only the zeros in the upper-half plane and on the real axis. We shall use the argument principle to determine the number and location (left or right half-plane) of these zeros. We adopt the terminology "complex zeros" to mean a zero with nonvanishing imaginary part.

Theorem 1: For any "single bumped" distribution F , A has no zeros for $\sigma^2 < 1$. (We do not consider the singular case $\sigma^2 = 1$ which represents zeros of A at ∞ .)

This result is well known.^{1,2} and in any event can be seen trivially from the appropriate Nyquist diagram for A .

^{a)}Supported in part by the National Science Foundation Grant Number ENG75-15882.

Suppose F has two bumps. We distinguish three cases for convenience.

Case 1: "Bump on left tail"; $F(u)$ is an ordinary Maxwellian with a bump for $u < 0$.

Case 2: "Bump on right tail"; $F(u)$ is an ordinary Maxwellian with a bump for $u > 0$.

Case 3: "Two stream"; $F(u)$ has one peak for $u < 0$, and one for $u > 0$.

In each case F' will vanish at three finite points. We call them $u_0 < u_1 < u_2$ (for Case 1, $u_2 \leq 0$; for Case 2, $u_0 \geq 0$; for Case 3 $u_0 < 0 < u_2$). Mathematically these three cases could be treated as one, but the above division helps clarify the physics. We need the following results;

Lemma 1: For $u > 0$, $\text{Im}A(iu) < 0$ in Case 1 and $\text{Im}A(iu) > 0$ in Case 2.

Proof: From Eq. (3),

$$\text{Im}A(iu) = u^3 \sigma^2 \int_{-\infty}^{\infty} \frac{F'(s)}{s^2 + u^2} ds. \quad (4)$$

For Case 1 the only contribution to the integral comes from the perturbing bump, call it F'_1 . Decompose F'_1 into its even and odd parts, F'_{1e} and F'_{1o} . Then only F'_{1e} contributes to the integral in Eq. (4). F'_{1e} will vanish at two points, $\pm y$, $y > 0$. Furthermore, $F'_{1e}(u) < 0$ for $|u| < y$ and $F'_{1e}(u) > 0$ for $|u| > y$. It is easily seen that the contribution to the integral in Eq. (4) is negative, since if we add

$$0 = \frac{-u^3 \sigma^2}{y^2 + u^2} \int_{-\infty}^{\infty} F'_{1e}(s) ds$$

to Eq. (4), we obtain

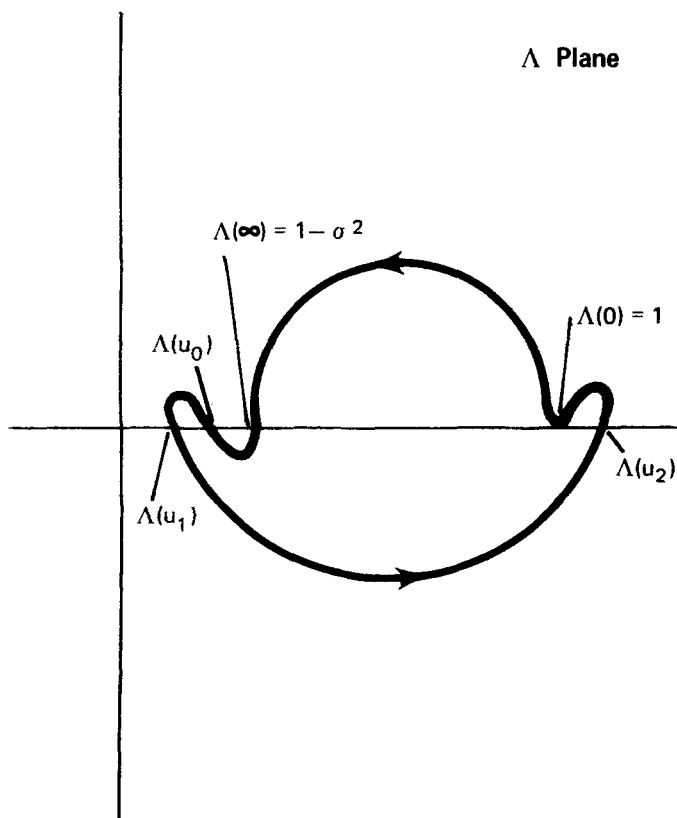


FIG. 1a. Nyquist diagram for Case 1, conditions 1a.

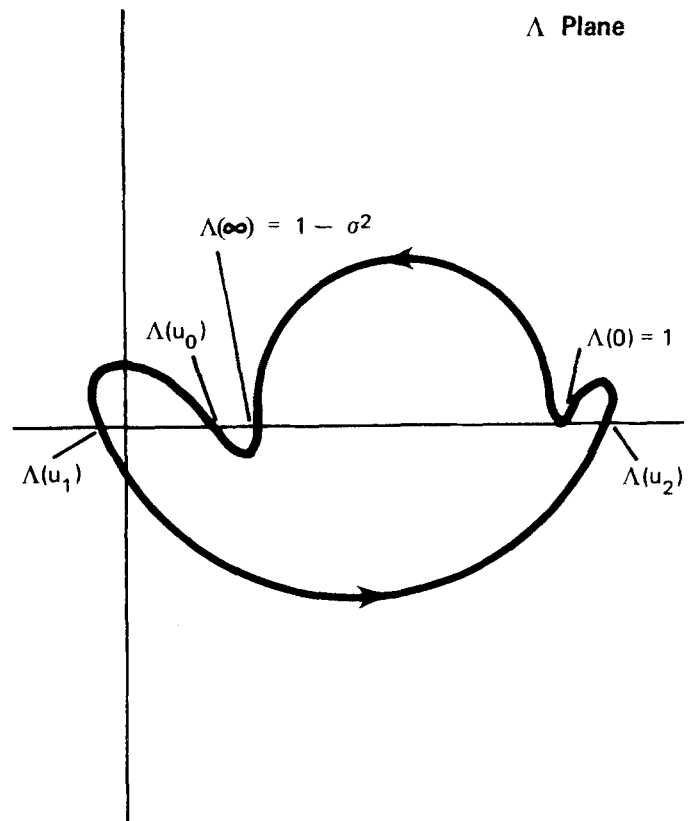


FIG. 1b. Nyquist diagram for Case 1, condition 1b.

$$\text{Im}A(iu) = u^3 \sigma^2 \int_{-\infty}^{\infty} \frac{(y^2 - s^2)F'_{1e}(s)}{(u^2 + s^2)(y^2 + u^2)} ds, \quad (5)$$

thus completing the proof of the Lemma for Case 1. Case 2 is analogous.

We now let $M = A(u_0)A(u_1)A(u_2)$. We then have **Theorem 2:**

1. $1 - \sigma^2 > 0$:

(a) $M > 0$; then for Case 1, 2 and 3, A has no zeros;

(b) $M < 0$, then, for Case 1, A has two zeros in the left half-plane; for Case 2, A has two zeros in the right half-plane; for Case 3, A has two zeros.

2. $1 - \sigma^2 < 0$:

(a) $M > 0$; for Case 1, A has two zeros in the right half-plane; for Case 2, A has two zeros in the left half-plane; for Case 3, A has two zeros;

(b) $M < 0$, for Cases 1 and 2, A has two zeros in both left and right half-planes; for Case 3, A has either no zeros or four zeros.

Proof: We draw the Nyquist diagram for $A(u)$ as u proceeds from $-\infty$ to $+\infty$ just above the real axis and closes in a semicircular arc in the upper half plane (along the semicircular arch, $A \sim 1 - \sigma^2 = \text{const}$, so that portion of the contour makes no change in the argument of A). From Eq. (3),

$$A^\pm(u) = \lim_{\epsilon \rightarrow 0^+} A(u \pm i\epsilon) = 1 - \sigma^2 u \int_{-\infty}^{\infty} \frac{sF'(s)}{s - u} ds \mp i\sigma^2 u^2 F'(u). \quad (6)$$

We show in Figs. 1a and 1b a Nyquist diagram corre-

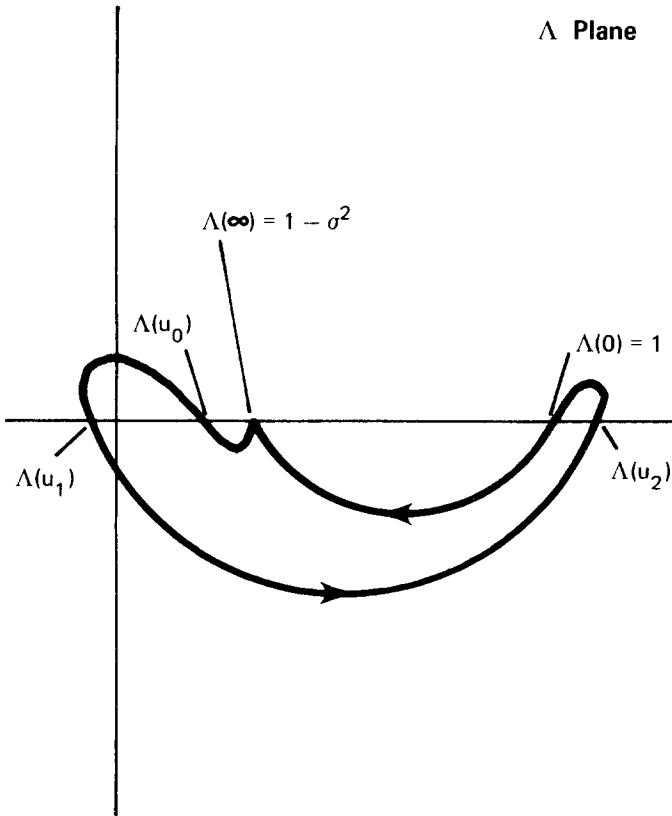


FIG. 2. Nyquist diagram for Case 1, condition 1b, mapping second quadrant only.

sponding to the situations stated in the theorem for Case 1. Note that from Eq. (6), the contour in the Λ plane crosses the real axis at $\pm \infty, u_1, u_2, u_0,$ and 0 and since Λ is analytic in the upper half-plane, we must insure that the bounded component of the Λ plane is to the left as one traverses the contour (otherwise the diagram obtained represents a function that has a pole in the upper half-plane). A brief perusal of these figures verifies the assertions of the theorem for Case 1 insofar as the number of zeros is concerned. To prove that the zeros are located in the stated half-plane, consider Lemma 1 and follow the curve in the Λ plane as u advances from $-\infty$ to 0 above the real axis, and from 0 to ∞ upward along the imaginary axis.

Using Lemma 1 we can draw the contour as in Fig. 2, showing that the root does indeed occur in the left half-plane, which completes the proof of the theorem.

The other possibilities for Case 1 are treated in an analo-

TABLE I. Zeros of Λ for perturbed Maxwellian. R(L)HP = right (left) half-plane.

	Case 1	Case 2
1. $1 - \sigma^2 < 0$		
a) $M > 0$	none	none
b) $M < 0$	2 in LHP	2 in RHP
2. $1 - \sigma^2 > 0$		
a) $M > 0$	2 in RHP	2 in LHP
b) $M < 0$	2 in RHP, 2 in LHP	2 in RHP, 2 in LHP

TABLE II. Zeros of Λ for Case 3.

1. $1 - \sigma^2 > 0$	
a) $M > 0$	none
b) $M < 0$	2 zeros
2. $1 - \sigma^2 < 0$	
a) $M > 0$	2 zeros
b) $M < 0$	none or 4 zeros

gous fashion. In the same way, Cases 2 and 3 can be analyzed. The results are summarized in Tables I and II. We note that real zeros can occur, but only at $u_0, u_1,$ or $u_2,$ where $\text{Im}\Lambda$ vanishes, or at ∞ in the special case $\sigma^2 = 1$.

III. FACTORIZATION OF Λ

For anisotropic plasmas, the factorization of Refs. 1 and 2 is not applicable to the equilibrium distribution functions we consider. We require

$$\Lambda(\rho) = X(\rho)Y(-\rho) \tag{7}$$

with X and Y analytic for $\text{Re}\rho < 0$. Furthermore, if we let ν_r and ν_l represent the zeros of Λ in the right and left half-planes respectively, then we also require

$$X(\nu_r) = 0 \quad \text{for } \text{Re}\nu_r > 0,$$

$$Y(-\nu_l) = 0 \quad \text{for } \text{Re}\nu_l < 0.$$

If Λ has no zeros, then the following functions are immediately seen to factor Λ :

$$X_0(\rho) = (1 - \sigma^2)^{1/2} \exp \left[\frac{1}{2\pi i} \int_0^\infty \ln \left(\frac{\Lambda^+(s)}{\Lambda^-(s)} \right) \frac{ds}{s - \rho} \right], \tag{8a}$$

$$Y_0(\rho) = (1 - \sigma^2)^{1/2} \times \exp \left[- \frac{1}{2\pi i} \int_0^\infty \ln \left(\frac{\Lambda^+(-s)}{\Lambda^-(-s)} \right) \frac{ds}{s - \rho} \right]. \tag{8b}$$

To include the zeros of Λ, X_0 and Y_0 must be modified

$$X_1(\rho) = (\rho - \nu_r)(\rho - \bar{\nu}_r) X_0(\rho), \tag{9a}$$

$$Y_1(-\rho) = (\rho - \nu_r)(\rho - \bar{\nu}_l) Y_0(-\rho), \tag{9a}$$

X_1 and Y_1 are still not adequate since $\Lambda(\rho) \rightarrow 1 - \sigma^2$ as $\rho \rightarrow \infty$ and the product $X_1(\rho)Y_1(-\rho)$ diverges as $\rho^n (n = 2$ or $4)$. Thus, X_1 and Y_1 must be modified to

$$X(\rho) = X_1(\rho)/\rho^{\epsilon_1}, \tag{10a}$$

$$Y(-\rho) = Y_1(-\rho)/\rho^{\epsilon_2}, \tag{10b}$$

where $\epsilon_1 (\epsilon_2)$ is either 2 or 0 depending on whether Λ does or does not have a zero in the right (left) half-plane.

To verify that X and Y have no pole at $\rho = 0$, we must determine the behavior of $X_0(0)$ and $Y_0(0)$. Since $\rho \sim 0$, the largest contribution in Eq. (8) comes from $s \sim 0$, so that we cut off the range of integration at, say, $a > 0$. Then a simple calculation shows for $\rho \rightarrow 0$

$$X_0(\rho) \sim \left(\frac{\rho - a}{\rho} \right)^{\theta_1(0)/\pi} \sim \rho^{-\theta_1(0)/\pi}, \tag{11a}$$

$$Y_0(\rho) \sim \left(\frac{\rho + a}{\rho} \right)^{-\theta_2(0)/\pi} \sim \rho^{\theta_2(0)/\pi}, \tag{11b}$$

TABLE III. Values of $\theta_1(0)$ and $\theta_2(0)$.

	Case 1	Case 2
1. $1 - \sigma^2 > 0$		
a) $M > 0$	$\theta_1(0) = 0$ $\theta_2(0) = 0$	$\theta_1(0) = 0$ $\theta_2(0) = 0$
b) $M < 0$	$\theta_1(0) = 0$ $\theta_2(0) = 2\pi$	$\theta_1(0) = -2\pi$ $\theta_2(0) = 0$
2. $1 - \sigma^2 < 0$		
a) $M > 0$	$\theta_1(0) = -2\pi$ $\theta_2(0) = 0$	$\theta_1(0) = 0$ $\theta_2(0) = 2\pi$
b) $M < 0$	$\theta_1(0) = -2\pi$ $\theta_2(0) = 2\pi$	$\theta_1(0) = -2\pi$ $\theta_2(0) = 2\pi$

where

$$\theta_1(s) = 1/2 \ln[A^+(s)/A^-(s)], \quad s > 0, \quad (11c)$$

$$\theta_2(s) = 1/2 \ln[A^+(-s)/A^-(-s)], \quad s > 0, \quad (11d)$$

We observe that

$$\begin{aligned} \theta_1(0) &= \Delta_{(0,\infty)} \arg A^+ \\ &= \Delta_{(0,\infty)} \arg A^+ + \Delta_{(0,+i\infty)} \arg A, \end{aligned}$$

where the second equality follows from Lemma 1. Similarly,

$$\begin{aligned} \theta_2(0) &= \Delta_{(-\infty,0)} \arg A^+ \\ &= \Delta_{(-\infty,0)} \arg A^+ + \Delta_{(0,+i\infty)} \arg A, \end{aligned}$$

where again we have used Lemma 1. Clearly, if the root occurs in the left half-plane, $\theta_1(0) = 0$ and $\theta_2(0) = 2\pi$, whereas if there is a root in the right half-plane, $\theta_1(0) = -2\pi$ and $\theta_2(0) = 0$. The results are summarized in Table III. Comparing these results with our definition of ϵ_1 and ϵ_2 , we have

$$\epsilon_1 = -\theta_1(0)/\pi, \quad (12a)$$

$$\epsilon_2 = \theta_2(0)/\pi, \quad (12b)$$

We see, incidentally, that the existence of a zero of A in the right or left half-plane induces a double zero in X_0 or Y_0 respectively, so that the notation in Eq. (9) is appropriate.

The result, Eq. (12), directly implies the following theorem.

Theorem 3: The functions X and Y defined by Eqs. (8), (9), and (10) constitute a Wiener-Hopf factorization of A given by Eq. (7) and

$$X(\rho) \sim \text{const} \quad \text{as } \rho \rightarrow 0.$$

$$Y(\rho) \sim \text{const} \quad \text{as } \rho \rightarrow 0.$$

Without loss of generality, we may set $X(0) = Y(0) = 1$.

IV. COUPLED NONLINEAR INTEGRAL EQUATIONS

For computational purposes, the explicit representation of X and Y obtained in the previous section may not be so convenient as the iterative solution of coupled integral equations. These may easily be determined from Cauchy's theorem. In particular, from Eq. (7)

$$X^+(u) - X^-(u) = \frac{1}{Y(-u)}$$

$$\times [A^+(u) - A^-(u)], \quad u > 0, \quad (13a)$$

$$\begin{aligned} &[Y(-u)]^+ - [Y(-u)]^- \\ &= \frac{1}{X(u)} [A^+(u) - A^-(u)], \quad u < 0. \end{aligned} \quad (13b)$$

Using Eq. (6) and the behavior of X and Y at infinity, Cauchy's theorem yields

$$X(\rho) = (1 - \sigma^2)^{1/2} - \int_0^\infty \frac{s^2 \sigma^2 F'(s)}{Y(-s)(s - \rho)} ds, \quad (14a)$$

$$Y(-\rho) = (1 - \sigma^2)^{1/2} - \int_{-\infty}^0 \frac{s^2 \sigma^2 F'(s)}{X(s)(s - \rho)} ds, \quad (14b)$$

These equations can be solved iteratively for the values of $X(\rho)$ and $Y(-\rho)$. A more convenient iteration scheme is defined by taking the limit as $\rho \rightarrow 0$ in Eqs. (14). Then

$$1 = (1 - \sigma^2)^{1/2} - \int_0^\infty s \sigma^2 F'(s) / Y(-s) ds, \quad (15a)$$

$$1 = (1 - \sigma^2)^{1/2} - \int_{-\infty}^0 s \sigma^2 F'(s) / X(s) ds, \quad (15b)$$

and rewriting Eq. (14) as

$$X(-\rho) = 1 + \rho \sigma^2 \int_0^\infty \frac{s F'(s)}{Y(-s)(s + \rho)} ds, \quad (16a)$$

$$Y(-\rho) = 1 - \rho \sigma^2 \int_0^\infty \frac{s F'(-s)}{X(-s)(s + \rho)} ds, \quad (16b)$$

If we make the following change of dependent variable,

$$U_1(\rho) = X^{-1}(-\rho) \rho \sigma^2 F'(-\rho), \quad (17a)$$

$$U_2(\rho) = -Y^{-1}(-\rho) \rho \sigma^2 F'(\rho), \quad (17b)$$

then Eqs. (14) reduce to the bilinear matrix equation

$$\mathbf{U} = \mathbf{F} + \mathbf{A}(\mathbf{U}, \mathbf{U}), \quad (18)$$

where

$$\mathbf{U} = [U_1, U_2], \quad (19a)$$

$$\mathbf{F}(\rho) = \rho \sigma^2 [F'(-\rho), -F'(\rho)], \quad (19b)$$

$\mathbf{A}(\mathbf{U}, \mathbf{V})(\rho)$

$$= \left[-\rho \int_0^\infty V_1(\rho) U_2(s) \frac{ds}{s + \rho}, \rho \int_0^\infty U_1(s) V_2(\rho) \frac{ds}{s + \rho} \right]. \quad (19c)$$

The convergence of the iteration scheme to Eq. (18) has been studied previously.⁴ If we define a Banach space with

$$\|\mathbf{U}\| = \max_{i=1,2} \int_0^\infty |U_i(s)| ds,$$

then it is shown by fixed point arguments that Eq. (18) has a unique solution in the ball

$$S = \{ \mathbf{U} : \|\mathbf{U} - \mathbf{F}\| < \frac{1}{2} \},$$

subject to the condition $\|\mathbf{F}\| < \frac{1}{2}$, and that an iteration scheme converges if the initial guess is chosen in S (note that if $\mathbf{U} \in S$, then $\|\mathbf{U}\| < 1$).

We now show that the solutions to Eq. (18) lying in S is the "physical" solution. We observe that U_1 and U_2 obey

$$U_1(\rho) = F_1(\rho) \left[1 + \int_0^\infty U_2(s) \frac{\rho}{s + \rho} ds \right]^{-1}, \quad (20a)$$

$$U_2(\rho) = F_2(\rho) \left[1 - \int_0^\infty U_1(s) \frac{\rho}{s+\rho} ds \right]^{-1}, \quad (20b)$$

Consider Case 1 for situation 1b of Table I. Then Y has zeros in the right half-plane which implies that U_2 has poles in the left half-plane. Thus U_2 must be analytic in the right half-plane and U_1 analytic in $\mathbb{C} \setminus [-\infty, 0]$. Since we are dealing with nonlinear integral equations which may have more than one solution, we must prove the following.

Theorem 4: For Case 1, $1 - \sigma^2 > 0$ and $M < 0$, the solution to Eq. (18), $[U_1, U_2]$, in the ball S , is analytic in the right half-plane.

Proof: Writing $\rho = \alpha x + i\beta$, we have

$$\left| \frac{\rho}{\rho+s} \right| = \left[\frac{\alpha^2 + \beta^2}{(\alpha+s)^2 + \beta^2} \right]^{1/2} < 1 \quad \text{for } 0 < s < \infty$$

and $\alpha > 0$;

thus

$$\left| \int_0^\infty U_{1,2}(s) \frac{\rho}{\rho+s} ds \right| < \int_0^\infty |U_{1,2}(s)| \left| \frac{\rho}{\rho+s} \right| ds < 1.$$

The result follows from Eq. (20).

To get a feeling for the range of parameters for which an iteration scheme corresponding to Eq. (18) converges, we have computed $\|F\|$ for a bump on tail distribution considered in Ref. 3 and given explicitly by

$$F(u) = (1-\beta) \left(\frac{m}{2\pi k T_1} \right)^{1/2} \exp\left(-\frac{mu^2}{2kT_1}\right) + \beta \left(\frac{m}{2\pi k T_2} \right)^{1/2} \exp\left[-\frac{m(u-V_0)^2}{2kT_2}\right]. \quad (21)$$

A straightforward integration yields

$$\|F\| \leq \sigma^2 \left[\frac{1}{2} - \frac{1}{2}\beta E_2 \left(\frac{mV_0^2}{2kT_2} \right)^{1/2} + 2\beta \left(\frac{mV_0^2}{2\pi k T_2} \right)^{1/2} \right], \quad (22)$$

where E_2 is the error function defined in Ref. 5. A more convenient, if less exact, bound is

$$\|F\| < \sigma^2 \left[\frac{1}{2} + 2\beta \left(\frac{mV_0^2}{2\pi k T_2} \right)^{1/2} \right]. \quad (23)$$

We conclude that, for certain values of σ^2 , β , V_0 , and T_2 , an iteration scheme converges if the initial guess is chosen in S . For values outside this range, it is necessary to evaluate X and Y from the explicit definitions. We now develop these definitions into a form more useful for computation by a procedure similar to one used in Ref. 2, p. 130.

From Eqs. (8), (9), and (10) we have

$$X(\rho) = (\rho - \nu_r)(\rho - \bar{\nu}_r) \rho^{-\epsilon_1} (1 - \sigma^2)^{1/2} \times \exp\left[\frac{1}{\pi} \int \frac{\theta(s)}{s-\rho} ds \right], \quad (24a)$$

$$Y(-\rho) = (\rho - \nu_l)(\rho - \bar{\nu}_l) \rho^{-\epsilon_2} (1 - \sigma^2)^{1/2} \times \exp\left[\frac{1}{\pi} \int_{-\infty}^0 \frac{\theta(s)}{s-\rho} ds \right], \quad (24b)$$

where

$$\theta(s) = \arg A^+(s) = \tan^{-1} \left[\frac{-\pi\sigma^2 s^2 F'(s)}{\lambda(s)} \right], \quad (25a)$$

$$\lambda(s) = \frac{1}{2} [A^+(s) + A^-(s)]. \quad (25b)$$

It is useful to write in Eq. (24)

$$\int_0^\infty \frac{\theta(s)}{s-\rho} ds = \int_0^\infty \theta(s) \frac{d}{ds} \ln(s-\rho) ds, \quad (26)$$

and, integrating by parts, we have

$$\int_0^\infty \frac{\theta(s)}{s-\rho} ds = \epsilon_1 \ln(-\rho) - \int_0^\infty \frac{d\theta}{ds} \ln(s-\rho) ds, \quad (27a)$$

$$\int_{-\infty}^0 \frac{\theta(s)}{s-\rho} ds = \epsilon_2 \ln(-\rho) - \int_{-\infty}^0 \frac{d\theta}{ds} \ln(s-\rho) ds. \quad (27b)$$

Here we have used Eq. (12) and the fact that $\theta(\infty) = 0$. Calculating $d\theta/ds$ from Eq. (25a) and using (24) and (27), we obtain after some algebra

$$X(\rho) = (\rho - \nu_r)(\rho - \bar{\nu}_r)(1 - \sigma^2)^{1/2} \times \exp\left\{ -\frac{1}{\pi} \int_0^\infty \text{Im} \left[\frac{A^+(s)}{A^+(s)} \right] \ln(s-\rho) ds \right\}, \quad (28a)$$

$$Y(-\rho) = (\rho - \nu_l)(\rho - \bar{\nu}_l)(1 - \sigma^2)^{1/2} \times \exp\left\{ -\frac{1}{\pi} \int_{-\infty}^0 \text{Im} \left[\frac{A^+(s)}{A^+(s)} \right] \ln(s-\rho) ds \right\}, \quad (28b)$$

We have proved that the Eq. (18) has a solution in the ball $S = \{V: \|V - F\| < \frac{1}{2} \text{ if } \|F\| < \frac{1}{2}\}$, which we now assume.

V. DISCUSSION

For computational purposes, we investigated the coupled nonlinear integral equation for X and Y in Sec. IV and found that, under certain restrictive conditions on the equilibrium distribution function, we could prove that an iteration scheme for the solution does converge. It might be possible to remove some of these conditions using other analytical techniques although thus far we have not been able to do so.

In Sec. III we found the Wiener-Hopf factorization of A , which is necessary in solving the half range problem using the Larsen and Habetler technique,⁶ as well as using techniques developed in Ref. 2. That is the problem we are currently pursuing.

¹F.C. Sure, Ph.D. Dissertation, University of Michigan, 1963.

²K.M. Case and P.F. Zweifel, *Linear Transport Theory* (Addison-Wesley, Reading, Mass., 1967).

³N.A. Krall and A.W. Trivelpiece, *Principles of Plasma Physics* (McGraw-Hill, New York, 1973).

⁴R.L. Bowden, R. Menikoff, and P.F. Zweifel, *J. Math. Phys.* **17**, 9 (1976).

⁵E. Jahnke and F. Emde, *Tables of Functions* (Dover, New York, 1945), p. 23.

⁶E.W. Larsen and G.J. Habetler, *Commun. Pure. Appl. Math.* **26**, 529 (1973).